Molecular Neurobiology (2019) 56:4894–4903
https://doi.org/10.1007/s12035-018-1399-8

Sirtuin3 Protected Against Neuronal Damage and Cycled into Nucleus in Status Epilepticus Model

Inja Cho[1,2] · Kyoung Hoon Jeong[1] · Jing Zhu[1] · Yun Ho Choi[1] · Kyoo Ho Cho[1] · Kyoung Heo[1] · Won-Joo Kim[1,2]

Received: 20 July 2018 / Accepted: 17 October 2018 / Published online: 8 November 2018

Abstract

In pathological conditions such as status epilepticus (SE), neuronal cell death can occur due to oxidative stress that is caused by an excessive production and accumulation of reactive oxygen species (ROS). Sirtuin3 (Sirt3) plays an important role in maintaining appropriate ROS levels by regulating manganese superoxide dismutase (MnSOD), which scavenges ROS in mitochondria. Using a SE model, we demonstrated that Sirt3 directly regulated MnSOD activity by deacetylation, which protects hippocampal cells against damage from ROS. Furthermore, we showed that after formation in the nucleus, Sirt3 is primarily located in the mitochondria, where it is activated and exerts its major function. Sirt3 then completed its pathway and moved back into the nucleus. Our data indicate that Sirt3 has an important function in regulating MnSOD, which results in decreased ROS in hippocampal cells. Sirt3 may have potential as an effective therapeutic target in SE conditions that would delay the progression of epileptogenesis.

Keywords Status epilepticus · Sirtuin3 · Manganese superoxide dismutase · Mitochondria · Nucleus

Introduction

Status epilepticus (SE) is an especially common emergency neurological condition that includes abnormally prolonged seizures and an increase in the amount of reactive oxygen species (ROS) produced. Accumulation of ROS is thought to play major roles in cell damage. In SE, ROS leads to oxidative stress-related neuronal cell death, which can give rise to chronic epilepsy and epileptogenesis [1–3]. In particular, the hippocampus is selectively vulnerable to stress, especially oxidative stress. This vulnerability is probably due to the connectivity of the subregions of the hippocampus, but the exact mechanism of ROS-induced stress has not been elucidated [4]. Under normal conditions, ROS is constantly produced as a modulator of cell signaling and is scavenged by antioxidant enzymes [e.g., manganese superoxide dismutase (MnSOD)] that are located in the mitochondria, which is a major site of ROS production. Hence, excessive ROS production caused by pathological conditions induces an imbalance between ROS production and the scavenging ability of antioxidants and results in oxidative stress [5, 6].

Sirtuin is a class III histone deacetylase that is an NAD^+-dependent protein deacetylase. Among the seven types of Sirtuin in mammalian species, which are classified by their location in the cellular compartment [7], the cellular function of Sirtuin 3 (Sirt3) has been identified in cardiac and metabolic disorders and aging [8–11]. The major functions of Sirt3 are to regulate mitochondrial electron transport chain activity, maintain ATP homeostasis by stimulating β-oxidation via deacetylation of long-chain acyl coenzyme A dehydrogenase [12], and regulate anti-oxidant enzymes and cell survival and longevity [9, 12, 13]. Recently, calorie restriction (CR) has been shown to extend life span and improve pathological conditions, and this phenomenon is related to the ability of Sirt3 to reduce oxidative stress. Indeed, previous studies have reported that Sirt3-mediated deacetylation of MnSOD (which contains nutrient- and ionizing radiation-dependent, hyperacetylated reversible acetyl-lysine), at Lys122 reduces oxidative stress and radiation in mice [14, 15]. In addition, mitochondrial Sirt3 has been shown to prevent age-related cochlea cell death

Electronic supplementary material The online version of this article (https://doi.org/10.1007/s12035-018-1399-8) contains supplementary material, which is available to authorized users.

✉ Won-Joo Kim
kzoo@yuhs.ac

[1] Department of Neurology and Epilepsy Research Institute, Yonsei University College of Medicine, 211 Eonju-ro, Gangnam-gu, Seoul, South Korea

[2] Brain Korea 21 PLUS Project for Medical Science, Yonsei University, Seoul, South Korea

due to oxidative stress [11, 16]. In contrast, Sirt3 deficiencies are associated with low levels of ATP and high levels of ROS, which can lead to diseases that have been linked to oxidative stress-related cell damage. Sirt3 has cell-protective properties related to the regulation of the anti-oxidant effect across diverse disease models, but the exact endogenous localization and the functional mechanism is considered controversial [17]. Moreover, although never reported in the literature, it is almost certain that Sirt3 has cell protective properties against oxidative stress in epilepsy. Thus, in the present study, we evaluated the role of Sirt3 against oxidative stress using a model of SE. Furthermore, we determined the endogenous location and alteration during SE of Sirt3 in hippocampal cells.

Materials and Methods

Animals and Pilocarpine-Induced SE Model

All procedures were approved by the Institutional Committee for the Care and Use of Laboratory Animals at Yonsei University Health System. Adult male C57BL/6 mice (20–25 g) and embryonic day 18 pregnant Sprague-Dawley rats (Orientbio, Gyeonggi, Korea) were used for in vivo and in vitro experiments, respectively. The animals were housed under a 12-h light/dark cycle and were given food and water ad libitum. SE was induced in mice by intraperitoneal (i.p.) injection of pilocarpine combined with methyl scopolamine (1 mg/kg; Sigma, St. Louis, MO, USA) to reduce peripheral cholinergic effects. After 30 min, mice were injected with pilocarpine hydrochloride (325 mg/kg, i.p.; Sigma) or the same volume of saline as a control. All animals treated with pilocarpine displayed motor seizures and exhibited onset of SE within 1 h. Only mice exhibiting sustained severe SE with generalized tonic and clonic movements after pilocarpine administration were included in the study ($n = 4$ or 5 in each group).

Primary Hippocampal Cell Culture

Whole hippocampal cells were obtained from the embryonic day 18 Sprague-Dawley rats, as described previously [18]. Briefly, embryos were transferred in ice-cold dissection medium composed of Hank's buffered salt solution (GIBCO-Invitrogen, Carlsbad, CA, USA) including 0.01 M 4-(2-hydroxyethyl)-1-piperazineethanesulfonic acid (HEPES), 100 U/ml penicillin, and 100 μg/ml streptomycin. The hippocampi were dissected and incubated with pre-warmed trypsin/ethylenediaminetetraacetic acid (EDTA) dissection medium at 37 °C for 12–15 min. Next, the hippocampi were titrated using a reverse-transcription polymerase chain reaction (RT-PCR), centrifuged for 5 min at 1000 rpm, and then resuspended in growth medium containing 2% B27 serum-free supplement, 0.5 mM GlutaMax supplement, 100 U/ml antipenicillin, and 100 μg/ml streptomycin (all from Invitrogen). Cells were plated on coated plates and then maintained in a humidified 5% CO_2 atmosphere at 37 °C for 2 weeks.

Small Interfering RNA Transfection, RNA Isolation, and RT-PCR

To detect Sirt3 positive bands in western blot analyses, small interfering RNA (si-RNA) and scrambled RNA (purchased from Santa Cruz Biotechnology, Dallas, TX, USA) were transfected with Lipofectamine RNAiMAX (Invitrogen) according to the manufacturer's protocol. After 3 days, total RNA was extracted from the transfected cultured hippocampal cells using Trizol reagent (Invitrogen), and cDNA was obtained using a SensiFAST cDNA Synthesis Kit (BIOLINE, London, UK) according to the manufacturer's instructions. Subsequently, 2 μ cDNA were used as a template for RT-PCR in an AccuPower® RT PreMix (Bioneer, Daijeon, Korea). The RT-PCR was performed using 10 pmol Sirt3 primer (Forward, 5'–TACTTCCTTCGGCTGCTTCA–3′; Reverse, 5'–AAGGCGAAATCAGCCACA–3′).

Mg^{2+}-Free Medium-Induced SE Condition

For the induction of SE, cultured cells were incubated with artificial cerebral spinal fluid (ACSF) medium without Mg^{2+} as described previously [18, 19]. Briefly, cultured hippocampal neurons (DIV 14–16) were rinsed with ice-cold phosphate-buffered saline (PBS) and then incubated with ACSF to equilibrate. After rinsing with ice-cold PBS, hippocampal cultured cells were incubated with Mg^{2+}-free external medium at 37 °C for 0 to 360 min.

Animal Tissue Preparation for Histological Assessment

Animals were anesthetized and perfused with heparinized saline. Following perfusion, the dorsal hippocampus was dissected and used immediately for western blot analysis and an activity assay. For histological analyses, brains were fixed with 3.7% formaldehyde in PBS after perfusion with heparinized saline and then isolated. In addition, brain tissue was post-fixed in the same fixative overnight at 4 °C and then sectioned using a cryostat. Cresyl violet staining was performed for histological assessment of hippocampal pyramidal damage. Sections were immersed in water and stained in 0.1% cresyl fast violet acetate for 5 min. The sections were then dipped well in absolute alcohol and rinsed with water, cleaned, and then mounted with mounting solution.

Fluorescent Labeling for DNA Fragmentation

To identify degenerating neurons, terminal deoxynucleotidyl transferase dUTP nick end labeling (TUNEL) staining was performed using a kit (Roche Diagnostics GmbH, Penzberg, Germany). Sections were incubated with the TUNEL mixture for 1 h at 37 °C in a dark chamber. After washing, the sections were counter-stained with Hoechst 33258 (2.5×10^{-3} mg/ml, Eugene, OR, USA) and examined under an LSM 700 confocal microscope (Carl Zeiss, Thornwood, NY, USA).

Immunofluorescence Staining for Hippocampal Tissue and Cultured Cells

Post-fixed brain tissues or cultured cells were blocked with PBS containing 5% bovine serum albumin for 1 h at room temperature and incubated with the primary antibody overnight. For a negative control, sections were also incubated without primary antibody. The sections were washed with PBS, and reacted with the fluorescence-conjugated secondary antibody (Jackson, West Grove, PA, USA) for 1 h at room temperature. The stained sections were observed using laser scanning (LSM 700 confocal microscopy).

Subcellular Fractionation and Western Blot Analysis

The mice hippocampus tissue was homogenized with Buffer A (Buffer A: 120 mM HEPES-KOH, 10 mM NaCl, 1.5 mM gCl2, 1 mM EDTA, 1 mM EDTA, 1 mM dithiothreitol, 250 mM sucrose), supplemented with protein inhibitor and 10 μM trichostatin A (TSA), and centrifuged at 750*g* for 10 min at 4 °C. After transferring the supernatant (containing mitochondria and cytosolic fraction) into a new tube, the pellet (nucleus) was resuspended in Buffer A containing 10% glycerol and 0.1% sodium dodecyl sulfate (SDS), centrifuged at 16,000*g* for 2 min at 4 °C, and then incubated for 30 min on ice. The supernatant (mitochondria/cytosolic fraction) was centrifuged at 10,000*g* for 5 min at 4 °C. The pellet (mitochondria) was resuspended in Buffer A. In the primary hippocampal cultured cells, a subcellular fraction was prepared using a Q proteome Cell Compartment Kit (Qiagen, Hilden, Germany) according to the manufacturer's protocol.

Immunoprecipitation Analysis

Cultured cells and hippocampal tissue were lysed in Tris-KOH buffer. Sirt3 or MnSOD antibodies were added to the lysates that were then incubated overnight at 4 °C. The following day, protein G sepharose beads (Invitrogen) were added, and the lysates were incubated for an additional 4 h at 4 °C. Then, the lysates with beads were spun down and washed with wash buffer. Immunoblot analysis of the lysates with beads was performed using 12% SDS-polyacrylamide gel electrophoresis (PAGE).

MnSOD Activity Assay

MnSOD activity was measured with a modified method as described by the commercial SOD Assay Kit (Dojindo Molecular Technologies, Rockville, MD, USA). The hippocampi were quickly dissected and homogenized in cold sucrose buffer (0.25 M sucrose, 10 mM Tris, 1 mM EDTA, pH 7.4) using a Teflon homogenizer. The homogenized tissue was centrifuged at 10,000*g* for 60 min at 4 °C. Diethyldithiocarbamate (final concentration: 1 mmol/l; Sigma), an SOD1 and SOD3 inhibitor, was added to the lysates, and the samples were assayed. The concentration of SOD and a colorimetric method were used. One unit of SOD activity was defined as the amount that reduced the absorbance at 450 nm by 50% inhibition.

Cell Viability Assay

A colorimetric MTS assay was performed using the CellTiter 96® AQ_{ueous} according to the manufacturer's protocol (Promega US, Madison, WI, USA). Briefly, CellTiter 96® AQ_{ueous} was added to cultured cells, which were plated in 24-well plates at 1/5 volume of the medium. Total absorption was measured using an enzyme-linked immunosorbent assay microplate reader (VersaMax, Molecular Devices, San Jose, CA, USA) at 490 nm at various time points.

Antibodies

The following antibodies were purchased: anti-Sirt3 (Santa Cruz Biotechnology, sc49744), anti-Sirt3 (abcam, ab86671), anti-acSOD (abcam, ab137037), anti-MnSOD (cell signaling, 13,141), MnSOD (Santa Cruz Biotechnology, sc18503), anti-coxIV (abcam, ab14744), anti-GAPDH (Santa Cruz Biotechnology, sc25778), anti-PARP (Santa Cruz Biotechnology, sc7150), anti-Lamin B (Santa Cruz Biotechnology, sc-6216), and β-actin (Santa Cruz Biotechnology, sc47778).

Statistical Analysis

Data are expressed as mean ± standard error. Statistical comparisons between multiple groups were made using ANOVA followed by Tukey's post hoc test (SPSS, version 5.01; SAS Institute Inc., Cary, NC, USA). Results between two independent groups were determined by a Mann-Whitney *U* test. The level of significance was set at $P < 0.05$.

Results

SE Induced Neuronal Cell Loss and Cell Death by Time Sequence in an In Vivo and In Vitro Model

We observed characteristic morphological changes in the hippocampus at various time points after inducing SE with pilocarpine in our model. Hippocampal cell alteration, such as shrinkage in the CA1 region, started 1 h after induction of SE. From 4 h after SE and onward, an apoptotic cell pattern was detected and hippocampal damage was observed consistently (Fig. 1a). We observed obvious apoptotic cells 12 h after induction of SE and these were markedly increased at 24 h. The number of damaged neurons stained with TUNEL correlated with the cresyl violet stating data (Fig. 1b). To confirm the in vitro results, we performed a cell viability test using a colorimetric MTS assay with primary hippocampal cells in a Mg^{2+}-free medium-induced SE condition. The cell viability was differentiated according to time sequence. At 3 h after induction of SE, cell viability decreased to around 70% (Fig. 1c). At 5 h after induction of SE, cell viability decreased to around 60% (Fig 1d, e). Based on these findings, we confirmed that SE precipitated hippocampal cell death both in vivo and in vitro.

Endogenous Sirt3 Localized Predominantly to Mitochondria in Hippocampal Cells

To investigate the endogenous Sirt3-specific positive band, we transfected primary hippocampal cells with si-Sirt3 or control si-RNA. The efficiency of Sirt3 knockdown was examined 72 h after si-RNA transfection. RT-PCR and western blot analysis showed a marked reduction in the level of Sirt3 (Fig. 2a). To investigate the location of endogenous Sirt3 in the hippocampus, we performed subcellular fractionation. Under subcellular fractionation analysis, the 28 kDa Sirt3 positive band was predominantly detected in the mitochondrial fraction, but a small amount of Sirt3 was detected in the nuclear fraction (Fig. 2b).

Mitochondrial Sirt3 Increased During Acute SE and Moved into the Nucleus

To determine the cause of the regulatory ability of Sirt3, we observed the alteration of Sirt3 at the cellular level by subcellular fractionation and immunostaining analysis. Subcellular fractionation revealed that at 40 min after SE, Sirt3 levels were higher in the mitochondria fraction than the control. At 90 min

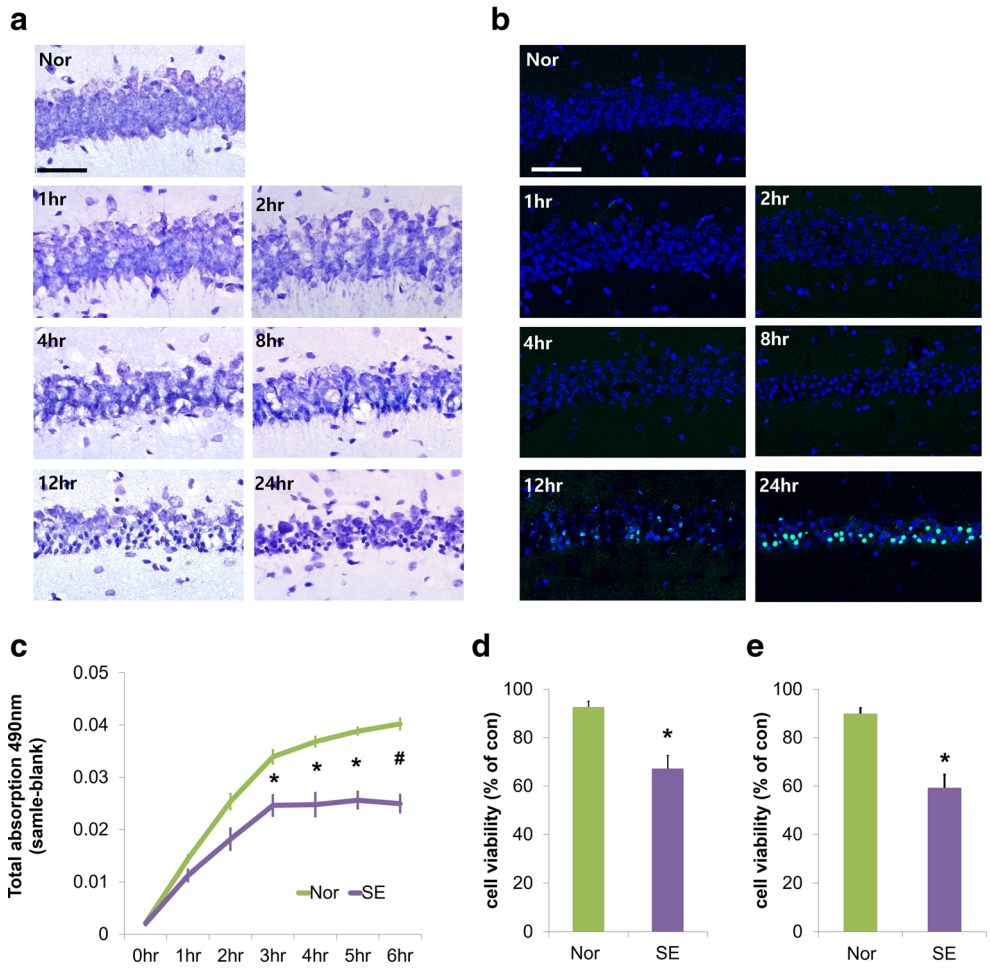

Fig. 1 Neuronal cell loss observed after induction of SE in in vivo and in vitro models. **a** Representative cresyl violet staining of hippocampal CA1 regions in control and SE-induced mice in vivo. Scale bar 50 μm. **b** Representative TUNEL (green) staining with Hoechst (blue) staining of hippocampal CA1 after induction of SE. Green indicates dead cells. Nor normal control; (1~24 h) 1~24 h after induction of SE. Scale bar 50 μm. **c** Total absorption of cell viability assay using CellTiter 96® AQ_{ueous} from hippocampal cultured cells from normal control and Mg^{+}-free-induced SE. **d**, **e** Results as percentage of relative normal control at 3 and 5 h after induction of SE. Data are presented as mean ± standard error. *) $P < 0.05$ vs. normal control, $^{\#}P < 0.001$ vs. normal control

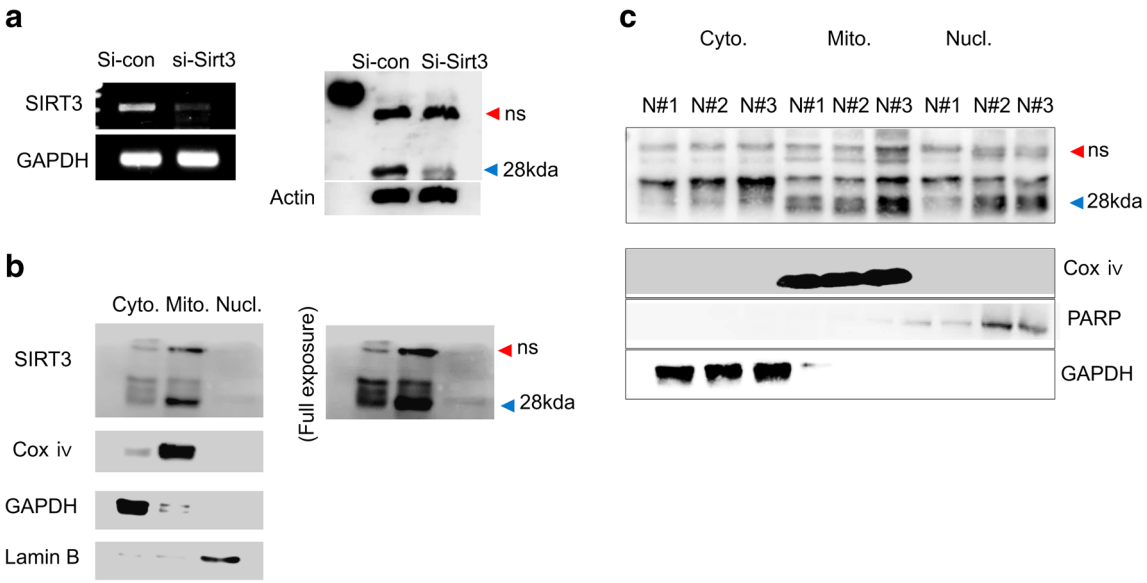

Fig. 2 Endogenous Sirt3 is predominantly located in mitochondria. **a** Observation of Sirt3 specific band using Sirt3 si-RNA. Left panel is polymerase chain reaction (PCR) and right is western blot analysis. A 28 kDa-specific Sirt3 band was detected in cultured hippocampal cells in the western blot data. **b** Subcellular fractionation analysis in normal hippocampal cultured cells. **c** Subcellular fractionation analysis in normal mice hippocampal tissue. Sirt3 was observed as a 28 kDa -specific band, which has some different modalities caused by different sensitivities of each antibody and is located in both the mitochondria and the nucleus. ns nonspecific band

after SE, there was not only a decrease of mitochondrial Sirt3, but also an increase of Sirt3 in the nuclear fractions (Fig. 3a). The Sirt3 immunostaining in hippocampal cultured cells revealed patterns that corresponded with the results of the subcellular fractionation analysis. We found co-staining of endogenous Sirt3 with MnSOD in normal controls, but co-staining with MnSOD and Sirt3 was increased compared to the control at 40 min after induction of SE. In contrast, at 90 min after induction SE, co-staining with MnSOD and Sirt3 had faded and the Sirt3 signal was exclusively recognized in the Hoechst region (Fig. 3b). The Sirt3 immunostaining in hippocampal tissue showed same pattern that corresponded with the pattern of hippocampal cultured cells (Fig. S1). These results provide evidence that during SE, after a transient increase of Sirt3 in the mitochondria, Sirt3 translocated to the nucleus.

Interaction Between Sirt3 and MnSOD Temporarily Increased During Acute SE

We investigated the interaction between Sirt3 and MnSOD from hippocampal cultured cells and tissue during SE. We discriminated positive bands using normal goat IgG as a negative control in immunoprecipitation analysis (Fig. 4a, b), indicating that Sirt3 directly interacted with MnSOD. The expression levels of MnSOD and Sirt3 in whole lysate were unchanged during SE (the levels showed a tendency to increase that was not significant). In contrast, acetylated MnSOD levels were significantly decreased 40 min after induction of SE in hippocampal cultured cells. At the same time point, the level of interaction between Sirt3 and MnSOD increased in hippocampal cultured cells (Fig. 4c, d). The decreased acetylated MnSOD level implies a relative increase of deacetylated MnSOD, which in turn, indicates an increase in MnSOD activity. These results correlate with the transient increase in interaction between Sirt3 and MnSOD that was detected 4 h after induction of SE in hippocampal tissue after that interaction level was decreased at the base level (Fig. 4e). Immunoprecipitation data were used to clarify whether Sirt3 regulated MnSOD activity by a direct interaction. Our evaluation of MnSOD activity revealed a transient increase in MnSOD activity, which was detected at the same time as the immunoprecipitation data (Fig. 4f). These results indicate that Sirt3 directly regulated MnSOD activity and that the interaction between Sirt3 and MnSOD temporarily increased in hippocampal cells at the acute time period during induction of SE. Moreover, the temporarily ability of Sirt3 to increase MnSOD activity was detected both in vitro and in vivo.

Sirt3 Deficiency Exacerbate Hippocampal Cell Vulnerability During SE Condition

We queried whether Sirt3 has a crucial role in progression of epileptic condition, we performed a cell viability assay with hippocampal cultured cell transfected with Sirt3 si RNA in a Mg^{2+}-free medium-induced SE condition. Before induction of SE, there was no significant

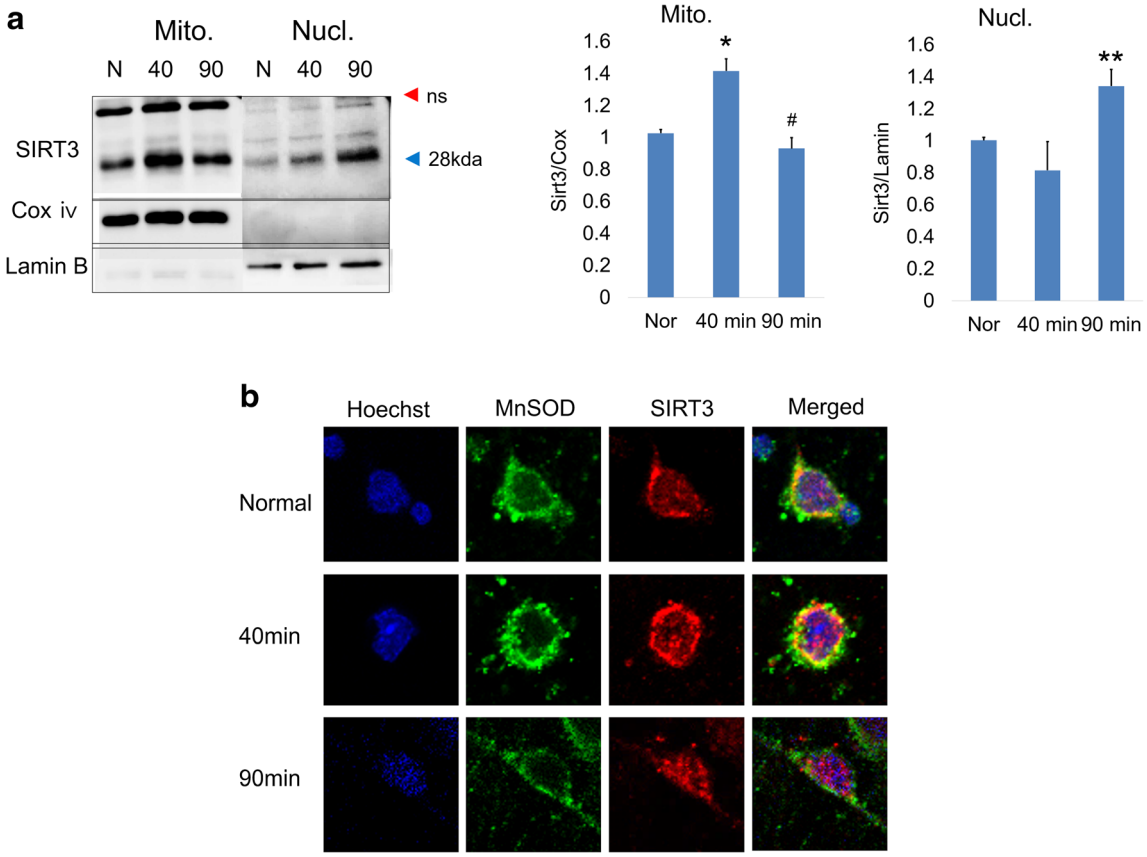

Fig. 3 Mitochondrial Sirt3 temporarily increased during acute SE. **a** Subcellular fractionation analysis in hippocampal cultured cells at normal (Nor), 40 min after induction of SE, and 90 min after induction of SE. Optical density data are presented as mean ± S.E. Key: $^{*}P < 0.05$ vs. the Nor, $^{\#}P < 0.001$ and $^{**}P < 0.05$ vs. 40 min post-SE induction. **b** Immunofluorescence staining with MnSOD, Sirt3, and Hoechst in hippocampal cells

difference between Control siRNA and Sirt3 si RNA-treated cells. At 5 h after induction of SE, Sirt3 si RNA -treated cells showed significant decrease cell viability rate compared to the Control siRNA-transfected cells (Fig. 5). These results indicated that Sirt3 deficiency promote hippocampal cell loss in SE condition.

Sirt3 Translocated to Nucleus from Mitochondria During Induction of SE

Our results suggest that Sirt3 translocated to the nucleus from the mitochondria during acute periods of SE induction. To determine whether the increase of nucleic Sirt3 was derived from mitochondria during SE, hippocampal cultured cells were treated with the nucleus import blocker importazole (IPZ, 100 mM; Sigma) for 50 min. At the 40-min time point following the Mg^{2+}-free medium-induction of SE, cells were treated with IPZ or DMSO for 50 min. The increase in nucleic Sirt3 was diminished by IPZ at 90 min in the SE group compared to the vehicle group (Fig. 6a). This result is consistent with our subcellular fractionation data observations. At 90 min after induction of SE, there was not only a decrease in mitochondrial Sirt3 but also an increase in nucleic Sirt3 compared with levels at 40 min after induction of SE. This increase in Sirt3 in the nucleic fraction was completely blocked by IPZ treatment and accompanied by a significant increase in Sirt3 in the non-nucleic fractions (Fig. 6b). Consequently, these data indicate that an increase in nucleic Sirt3 may have migrated from the mitochondria.

We next observed hippocampal cells that were treated with Lapamycin B (LMB, 20 nM; Santa Cruz), a nuclear export inhibitor, to clarify Sirt3 translocation from the mitochondria to the nucleus. Initially, at the start of inducing the epileptic condition, cells were treated with LMB or EtOH (for vehicle) for 40 min. Although examination of Sirt3 staining revealed no differences in the vehicle-treated cells, the mitochondrial Sirt3 declined following LMB treatment and increased in the nucleic pattern of Sirt3 at 40 min after induction of SE (Fig. 6c). Moreover, the level of nucleic Sirt3 detected did not differ from the cells treated with LMB at 90 min after SE (Fig. 6D). This result indicates that the increased mitochondrial Sirt3 transferred from the nucleus after induction of SE and then mitochondrial Sirt3 translocated to the nucleus as the development of SE progressed.

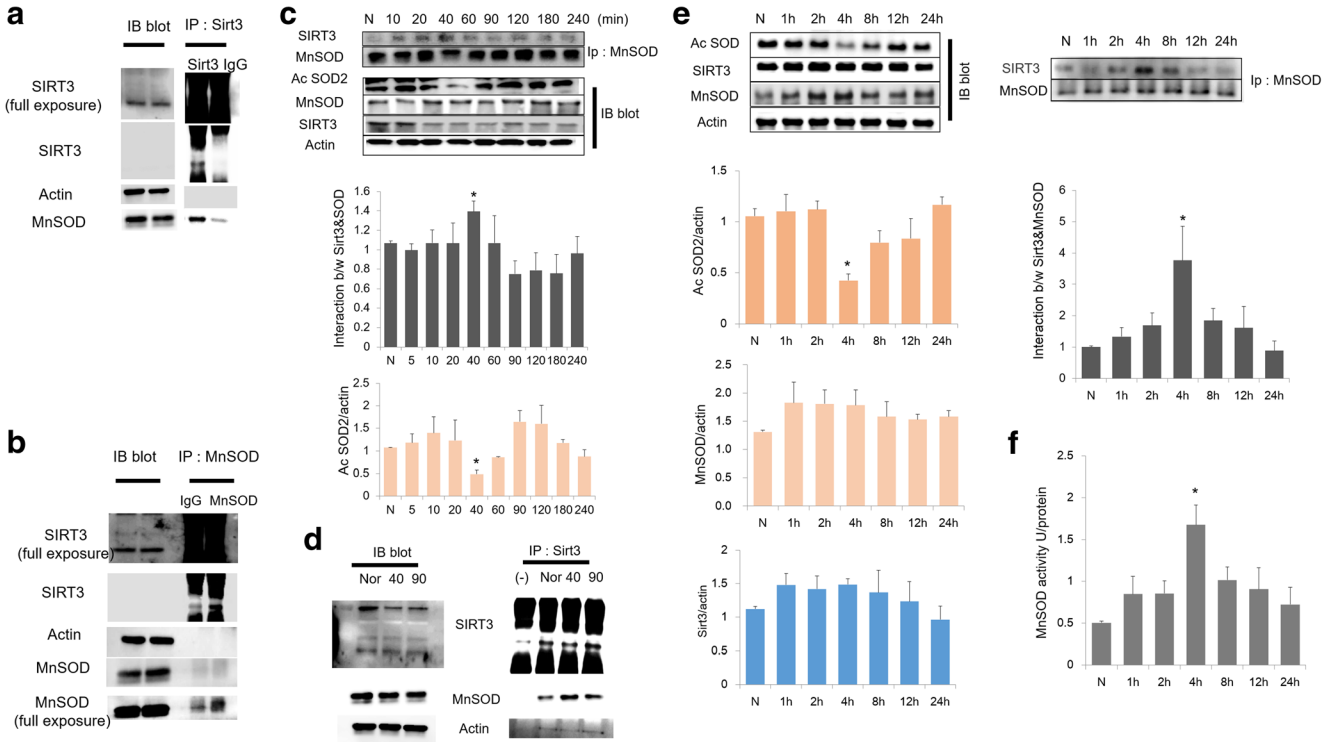

Fig. 4 Interaction between MnSOD and Sirt3 temporarily increased during acute SE in vitro. **a**, **b** Protein from primary hippocampal cultured cells was immunoprecipitated with MnSOD or Sirt3 and goat IgG was used as a negative control. **c**, **d** Alteration of interaction between MnSOD and Sirt3 after inducing Mg^{+}-free induced SE. The interacting protein level was expressed using optical density. An increase of interaction between MnSOD and Sirt3 was detected at 40 min after induction of SE. At the same time, the deacetylated MnSOD level was also significantly increased. **e** Hippocampal tissue immunoprecipitated with MnSOD. **f** MnSOD activity assay from hippocampal tissue at various time points after induction of SE

Discussion

The present study demonstrated that Sirt3 directly regulated MnSOD activity and transiently increased MnSOD activity via the deacetylation that occurs during acute SE development in hippocampal cells. We also found that endogenous hippocampal Sirt3, which is predominantly located in mitochondria, was transiently increased in the mitochondria and then translocated to the nucleus during an acute SE phase. This pattern correlated with altered MnSOD activity during SE. These results suggest that Sirt3 changed location and that the regulatory ability of Sirt3 against oxidative stress via MnSOD deacetylation in hippocampal cells may be influenced by where they are located during acute SE.

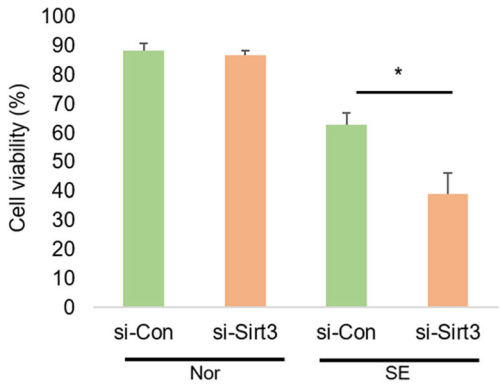

Fig. 5 Sirt3 deficiency exacerbate hippocampal cell loss during SE in vitro. Cell viability assay in hippocampal cultured cells transfected with Control si RNA or Sirt3 si RNA-treated cells from Mg^{+}-free-induced SE. Nor, normal condition; SE, Mg2 + −free medium-induced SE condition. Data are presented as mean ± standard error. $*P < 0.05$ vs. Con siRNA

Many studies implicate oxidative stress as a cause of diverse diseases, including neurodegenerative disorders. Accumulation of ROS induces homeostatic imbalance between antioxidant enzymes, and the generation of oxidative stress is involved in a critical step of pathogenesis [20, 21]. MnSOD, which is also known to be located in mitochondria, is one of the major antioxidant defense systems against oxidative stress [22]. Previous studies have demonstrated that MnSOD overexpression exerts a cell protective effect and prolongs life span by ameliorating oxidative stress [23]. In kainate-induced hippocampal damaged mice models and Alzheimer's disease models, an overexpression of MnSOD has been shown to provide neuronal cell protection against oxidative stress [24, 25]. In contrast, knock-out of MnSOD has been shown to lead to early death, indicating the

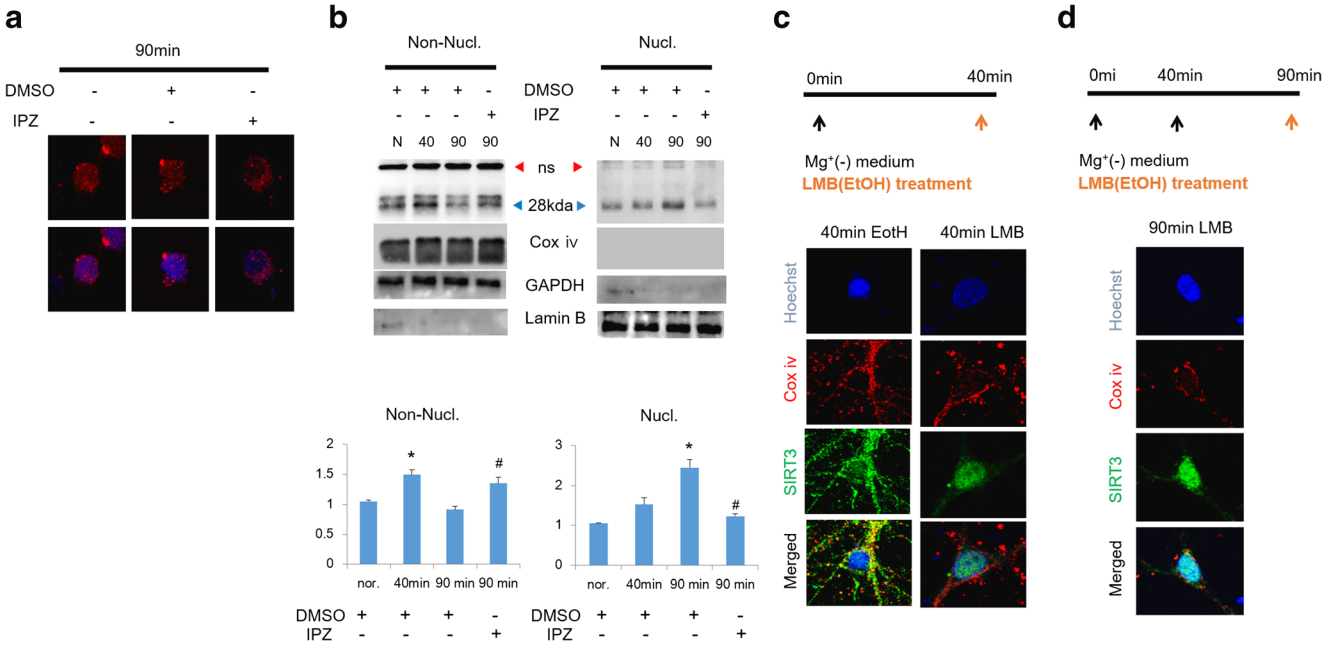

Fig. 6 Sirt3 translocated to nucleus from mitochondria during SE. **a** Cells treated with importazole (IPZ; 100 μM), as a nuclear import blocker, at normal and 90 min after induction of SE. **b** Subcellular fractionation data in hippocampal cultures cells treated with IPZ. Optical density is presented as mean ± standard error. $^{*}P < 0.05$ vs. the normal (Nor) cells treated with DMSO; $^{**}P < 0.05$ vs. the 40 min SE cells treated with DMSO; $^{\#}P < 0.001$ vs. the 90-min SE cells treated with DMSO. **c** Cells treated with Lapamycin B (LMB; 20 nM), as a nuclear export blocker, at normal and 40 min after induction of SE. **d** Cells treated with Lapamycin B (LMB; 20 nM), as a nuclear export blocker, at normal and at 90 min after induction of SE

mechanism seems to reduce mitochondrial activity in the central nervous system [26, 27]. Deficiency of MnSOD results in severe seizures that precipitate nerve system degeneration [28]. Therefore, a therapeutic strategy to inhibit oxidative stress by regulating MnSOD activity has been suggested for diverse disease groups. In our results, MnSOD activity began to increase 1 h after SE (although not significantly), peaked at 4 h after SE, and decreased to around the basal level during SE. Previously, it was reported that SE and other epileptogenic injuries cause accumulation of ROS in acute periods [3]. Therefore, transiently increased MnSOD activity is regarded as scavenging for ROS to protect the cells from oxidative stress during the acute phase of SE.

A recent study reported that Sirt3 regulates MnSOD via deacetylation of the Lys 122 residue, protecting against oxidative stress by CR [14, 15]. In addition, several studies have provided evidence for the cell protective effects of Sirt3 in diverse cell types, including cardiomyocytes, pancreatic cells, and cortical neurons [29–32]. Interestingly, these protective effects have been shown to be related to the upregulation of the antioxidant ability and Sit3 regulates antioxidant protein via direct interaction [11, 33, 34]. Indeed, we also observed Sirt3 deficiency exacerbate cell death in hippocampal cultured cell in a Mg^{2+}-free medium-induced SE condition (Fig. 5). We also observed a direct interaction between Sirt3 and MnSOD that caused an MnSOD activity alteration. In addition, we observed the translocation of Sirt3 from the mitochondria to the nucleus during the acute SE phase. In accordance with an increase of MnSOD activity and interaction with Sirt3, an increase of Sirt3 was detected in the mitochondria. Concomitant with the decline of MnSOD activity and interaction with Sirt3, we observed an increase in nucleic Sirt3, which was confirmed by cells treated with IPZ and LMB.

Although initial reports suggest that Sirt3 is localized in the mitochondria [35–38], others have suggested that Sirt3 is also located in the nucleus [31, 33, 39–43]. In addition, Sirt3 has two isoforms (full-length and short- length, which is the N-terminal sequence truncated form), and their localization and cellular function remain controversial [17]. Nevertheless, the majority of studies have provided evidence that mitochondria Sirt3 exerts antioxidant activity against oxidative stress in diverse cell types. For example, in cardiomyocytes, Sirt3 was demonstrated to ameliorate oxidative stress and prevent oxidative stress-related apoptosis via the NF-κB pathway [29]. In cortical neurons, Sirt3 was shown to reduce numerous ROS that were the result of excitatory injury. On the other hand, the exact endogenous Sirt3 localization and its functional mechanism are considered controversial. We also demonstrated that Sirt3 is located not only in the mitochondria but also in the nucleus. Although we were unable to detect full-length Sirt3, we observed 28 kDa Sirt3 primarily located in the mitochondria in hippocampal cells and in nucleus in relatively small amounts. Previous studies provided evidence that Sirt3 is located in the mitochondria by using C-terminal detecting antibodies, and others demonstrated

that Sirt3 is located in the nucleus by using N-terminal antibody-detecting Sirt3, via recombinant green fluorescent protein-fused or overexpressed epitope-tagged Sirt3 [39, 41]. Although, the C-terminal detecting antibodies should be able to detect full-length and short-length Sirt3, we showed only 28 kDa Sirt3. This result suggests that full-length Sirt3 might be in relatively low abundance and an unstable form in contrast to mitochondrial Sirt3 [41]. In addition, some of discrepancy of detection is likely due to differences in the sensitivities of the antibodies. To confirm detection of a positive band without any non-specific bands, we performed si-RNA transfection and observed only the 28 kDa positive band. Consequently, our data demonstrate that Sirt3 is not only dominantly located in the mitochondria, it is also located in the nucleus at basal level. In addition, the quantity of nucleic Sirt3 increased following a mitochondrial Sirt3 transient increase for regulation of MnSOD activity during an acute SE phase.

Some studies reported that that full-length Sirt3 is located not only in the mitochondria but also in the nucleus [33, 39–41] and it transports to the mitochondria from the nucleus under stressful conditions. Moreover, C-terminal epitope-tagged Sirt3 has been detected in the nucleus before it translocates to the mitochondria [39]. Although there has been some controversy, we need to clarify whether increased Sirt3 in the nucleus is fallout from an accumulation of Sirt3 translocated from the mitochondria or interrupted protein that is going to translocate into the mitochondria. Consistent with previous reports, immunofluorescence of Sirt3 staining treated with LMB, as a nuclear export blocker, revealed no difference between EtOH and LMB groups under normal control conditions. In contrast, the increase of mitochondrial Sirt3 diminished in concurrence with a markedly increased nucleic pattern of Sirt3 after SE. These findings indicate that Sirt3 translocated to the mitochondria under stressful conditions. Moreover, 90 min after SE, elevated levels of nucleic Sirt3 did not differ from the cells treated with LMB and was decreased by IPZ treatment. These results suggest that Sirt3 translocated to the nucleus following an increase in the mitochondria during an acute SE phase.

Although the exact mechanisms of Sirt3 translocation to the nucleus are unknown and need further study, possible evidence exists. Sirt3 translocating to the nucleus from the mitochondria is not a novel finding. Previous studies have shown that when Sirt3 and Sirt5 co-expressed, the location of Sirt3 changed from the mitochondria to the nucleus as evidenced by disrupting the nuclear localization sequence. These findings suggest that Sirt3 may also play a role as a nuclear protein regulator [40]. Consistent with this report, we observed Sirt3 translocation to the nucleus from the mitochondria. Importantly, it is meaningful that in our study it was endogenous Sirt3 that translocated, and it was the first time this translocation was observed in a pathological condition. The exact role of nucleic Sirt3 in epileptic conditions will be the subject of our future investigations. Nevertheless, for the therapeutic implications, we would like suggest that consistent interaction between Sirt3 and MnSOD or upregulation of Sirt3 in mitochondria may have effective therapeutic target potential in SE conditions and delay the progression of epileptogenesis by ameliorating oxidative stress.

In summary, we found that Sirt3 deficiency exacerbate hippocampal cell loss in epileptic condition. In addition, during an acute SE period, Sirt3 translocated to the nucleus following an increase in mitochondria in hippocampal neuron cells that affected MnSOD activity. These results suggest that not only full-length Sirt3 but also 28 kD Srt3 has regulatory effects for nuclear protein via deacetylation. Although the mechanism of Sirt3 during SE is not yet understood and needs further studies to illuminate the process, we suggest that Sirt3 is crucial for regulating oxidative stress during acute SE phase that drives hippocampal loss and may lead to potential therapeutic target for protecting epileptogenesis after SE status.

Funding Information This study was supported by the Basic Science Research Program through the National Research Foundation of Korea funded by the Ministry of Education (NRF-2015R1D1A1A01059901) and by the Brain Korea 21 PLUS Project for Medical Science, Yonsei University.

References

1. Trinka E, Cock H, Hesdorffer D et al (2015) A definition and classification of status epilepticus–Report of the ILAE Task Force on Classification of Status Epilepticus. Epilepsia 56(10):1515–1523. https://doi.org/10.1111/epi.13121
2. Trinka E, Hofler J, Zerbs A (2012) Causes of status epilepticus. Epilepsia 53(Suppl 4):127–138. https://doi.org/10.1111/j.1528-1167.2012.03622.x
3. Waldbaum S, Patel M (2010) Mitochondrial dysfunction and oxidative stress: a contributing link to acquired epilepsy? J Bioenerg Biomembr 42(6):449–455. https://doi.org/10.1007/s10863-010-9320-9
4. Geddes DM, LaPlaca MC, Cargill RS 2nd (2003) Susceptibility of hippocampal neurons to mechanically induced injury. Exp Neurol 184(1):420–427
5. Murphy MP (2009) How mitochondria produce reactive oxygen species. Biochem J 417(1):1–13. https://doi.org/10.1042/BJ20081386
6. Schieber M, Chandel NS (2014) ROS function in redox signaling and oxidative stress. Curr Biol 24(10):R453–R462. https://doi.org/10.1016/j.cub.2014.03.034
7. Michan S, Sinclair D (2007) Sirtuins in mammals: insights into their biological function. Biochem J 404:1–13. https://doi.org/10.1042/Bj20070140
8. Duan W (2013) Sirtuins: from metabolic regulation to brain aging. Front Aging Neurosci 5:36. https://doi.org/10.3389/fnagi.2013.00036
9. Ahn BH, Kim HS, Song S et al (2008) A role for the mitochondrial deacetylase Sirt3 in regulating energy homeostasis. Proc Natl Acad Sci U S A 105(38):14447–14,452. https://doi.org/10.1073/pnas.0803790105
10. Sundaresan NR, Gupta M, Kim G, Rajamohan SB, Isbatan A, Gupta MP (2009) Sirt3 blocks the cardiac hypertrophic response by augmenting Foxo3a-dependent antioxidant defense mechanisms in mice. J Clin Invest 119(9):2758–2771. https://doi.org/10.1172/JCI39162

11. Someya S, Yu W, Hallows WC et al (2010) Sirt3 mediates reduction of oxidative damage and prevention of age-related hearing loss under caloric restriction. Cell 143(5):802–812. https://doi.org/10.1016/j.cell.2010.10.002
12. Hirschey MD, Shimazu T, Goetzman E et al (2010) SIRT3 regulates mitochondrial fatty-acid oxidation by reversible enzyme deacetylation. Nature 464(7285):121–125. https://doi.org/10.1038/nature08778
13. Brown K, Xie S, Qiu X et al (2013) SIRT3 reverses aging-associated degeneration. Cell Rep 3(2):319–327. https://doi.org/10.1016/j.celrep.2013.01.005
14. Tao R, Coleman MC, Pennington JD et al (2010) Sirt3-mediated deacetylation of evolutionarily conserved lysine 122 regulates MnSOD activity in response to stress. Mol Cell 40(6):893–904. https://doi.org/10.1016/j.molcel.2010.12.013
15. Qiu X, Brown K, Hirschey MD, Verdin E, Chen D (2010) Calorie restriction reduces oxidative stress by SIRT3-mediated SOD2 activation. Cell Metab 12(6):662–667. https://doi.org/10.1016/j.cmet.2010.11.015
16. Quan Y, Xia L, Shao J et al (2015) Adjudin protects rodent cochlear hair cells against gentamicin ototoxicity via the SIRT3-ROS pathway. Sci Rep 5:8181. https://doi.org/10.1038/srep08181
17. Hallows WC, Albaugh BN, Denu JM (2008) Where in the cell is SIRT3?–functional localization of an NAD + −dependent protein deacetylase. Biochem J 411(2):e11–e13. https://doi.org/10.1042/BJ20080336
18. Cho YJ, Kim H, Kim WJ et al (2017) Trafficking patterns of NMDA and GABAA receptors in a Mg(2+)-free cultured hippocampal neuron model of status epilepticus. Epilepsy Res 136:143–148. https://doi.org/10.1016/j.eplepsyres.2017.08.003
19. Goodkin HP, Yeh JL, Kapur J (2005) Status epilepticus increases the intracellular accumulation of GABAA receptors. J Neurosci 25(23):5511–5520. https://doi.org/10.1523/JNEUROSCI.0900-05.2005
20. Waldbaum S, Patel M (2010) Mitochondria, oxidative stress, and temporal lobe epilepsy. Epilepsy Res 88(1):23–45. https://doi.org/10.1016/j.eplepsyres.2009.09.020
21. Lin MT, Beal MF (2006) Mitochondrial dysfunction and oxidative stress in neurodegenerative diseases. Nature 443(7113):787–795. https://doi.org/10.1038/nature05292
22. Birben E, Sahiner UM, Sackesen C, Erzurum S, Kalayci O (2012) Oxidative stress and antioxidant defense. World Allergy Organ J 5(1):9–19. https://doi.org/10.1097/WOX.0b013e3182439613
23. Holley AK, Dhar SK, Xu Y, St Clair DK (2012) Manganese superoxide dismutase: beyond life and death. Amino Acids 42(1):139–158. https://doi.org/10.1007/s00726-010-0600-9
24. Sompol P, Ittarat W, Tangpong J et al (2008) A neuronal model of Alzheimer's disease: an insight into the mechanisms of oxidative stress-mediated mitochondrial injury. Neuroscience 153(1):120–130. https://doi.org/10.1016/j.neuroscience.2008.01.044
25. Liang LP, Ho YS, Patel M (2000) Mitochondrial superoxide production in kainate-induced hippocampal damage. Neuroscience 101(3):563–570
26. Xu Y, Miriyala S, Fang F et al (2015) Manganese superoxide dismutase deficiency triggers mitochondrial uncoupling and the Warburg effect. Oncogene 34(32):4229–4237. https://doi.org/10.1038/onc.2014.355
27. Li H, Kantoff PW, Giovannucci E et al (2005) Manganese superoxide dismutase polymorphism, prediagnostic antioxidant status, and risk of clinical significant prostate cancer. Cancer Res 65(6):2498–2504. https://doi.org/10.1158/0008-5472.CAN-04-3535
28. Oh SS, Sullivan KA, Wilkinson JE et al (2012) Neurodegeneration and early lethality in superoxide dismutase 2-deficient mice: a comprehensive analysis of the central and peripheral nervous systems. Neuroscience 212:201–213. https://doi.org/10.1016/j.neuroscience.2012.03.026
29. Chen CJ, Fu YC, Yu W, Wang W (2013) SIRT3 protects cardiomyocytes from oxidative stress-mediated cell death by activating NF-kappaB. Biochem Biophys Res Commun 430(2):798–803. https://doi.org/10.1016/j.bbrc.2012.11.066
30. Kim M, Lee JS, Oh JE et al (2015) SIRT3 Overexpression Attenuates Palmitate-Induced Pancreatic beta-Cell Dysfunction. PLoS One 10(4):e0124744. https://doi.org/10.1371/journal.pone.0124744
31. Kim SH, Lu HF, Alano CC (2011) Neuronal Sirt3 protects against excitotoxic injury in mouse cortical neuron culture. PLoS One 6(3):e14731. https://doi.org/10.1371/journal.pone.0014731
32. Ren JH, Chen X, Zhou L et al (2016) Protective Role of Sirtuin3 (SIRT3) in Oxidative Stress Mediated by Hepatitis B Virus X Protein Expression. PLoS One 11(3):e0150961. https://doi.org/10.1371/journal.pone.0150961
33. Sundaresan NR, Samant SA, Pillai VB, Rajamohan SB, Gupta MP (2008) SIRT3 is a stress-responsive deacetylase in cardiomyocytes that protects cells from stress-mediated cell death by deacetylation of Ku70. Mol Cell Biol 28(20):6384–6401. https://doi.org/10.1128/MCB.00426-08
34. Cheng A, Yang Y, Zhou Y et al (2016) Mitochondrial SIRT3 Mediates Adaptive Responses of Neurons to Exercise and Metabolic and Excitatory Challenges. Cell Metab 23(1):128–142. https://doi.org/10.1016/j.cmet.2015.10.013
35. Schwer B, North BJ, Frye RA, Ott M, Verdin E (2002) The human silent information regulator (Sir)2 homolog hSIRT3 is a mitochondrial nicotinamide adenine dinucleotide-dependent deacetylase. J Cell Biol 158(4):647–657. https://doi.org/10.1083/jcb.200205057
36. Onyango P, Celic I, McCaffery JM, Boeke JD, Feinberg AP (2002) SIRT3, a human SIR2 homolog, is an NAD-dependent deacetylase localized to mitochondria. Proc Natl Acad Sci U S A 99(21):13653–13,658. https://doi.org/10.1073/pnas.222538099
37. Lombard DB, Alt FW, Cheng HL et al (2007) Mammalian Sir2 homolog SIRT3 regulates global mitochondrial lysine acetylation. Mol Cell Biol 27(24):8807–8814. https://doi.org/10.1128/MCB.01636-07
38. Cooper HM, Spelbrink JN (2008) The human SIRT3 protein deacetylase is exclusively mitochondrial. Biochem J 411(2):279–285. https://doi.org/10.1042/BJ20071624
39. Scher MB, Vaquero A, Reinberg D (2007) SirT3 is a nuclear NAD + −dependent histone deacetylase that translocates to the mitochondria upon cellular stress. Genes Dev 21(8):920–928. https://doi.org/10.1101/gad.1527307
40. Nakamura Y, Ogura M, Tanaka D, Inagaki N (2008) Localization of mouse mitochondrial SIRT proteins: shift of SIRT3 to nucleus by co-expression with SIRT5. Biochem Biophys Res Commun 366(1):174–179. https://doi.org/10.1016/j.bbrc.2007.11.122
41. Iwahara T, Bonasio R, Narendra V, Reinberg D (2012) SIRT3 functions in the nucleus in the control of stress-related gene expression. Mol Cell Biol 32(24):5022–5034. https://doi.org/10.1128/MCB.00822-12
42. Bao J, Lu Z, Joseph JJ et al (2010) Characterization of the murine SIRT3 mitochondrial localization sequence and comparison of mitochondrial enrichment and deacetylase activity of long and short SIRT3 isoforms. J Cell Biochem 110(1):238–247. https://doi.org/10.1002/jcb.22531
43. Salvatori I, Valle C, Ferri A, Carri MT (2017) SIRT3 and mitochondrial metabolism in neurodegenerative diseases. Neurochem Int 109:184–192. https://doi.org/10.1016/j.neuint.2017.04.012